Resolution of Maxwell's fisheye with an optimal active drain

Tomáš Tyc[1] **and Aaron Danner**[2]

[1] Faculty of Science and Faculty of Informatics, Masaryk University, Kotlářská 2, 61137 Brno, Czech Republic
[2] Department of Electrical and Computer Engineering, National University of Singapore, 117583 Singapore
E-mail: tomtyc@physics.muni.cz

Abstract

We analyse the resolution of Maxwell's fisheye in terms of the efficiency with which a pulse emitted from one point (source) can be absorbed at another point (drain) that is slightly displaced from the position of the image of the source. The drain is active and is designed to absorb the maximum possible amount of energy emitted by the source. Based on the size of the area where the energy can be absorbed efficiently, we address the question of whether such an active drain can provide subwavelength resolution and show that the answer is negative because this area is diffraction limited. We support our theoretical results with numerical simulations.

S Online supplementary data available from stacks.iop.org/njp/16/063001/mmedia

1. Introduction

Maxwell's fisheye (MFE) [1] and Maxwell's fisheye mirror [2–4] are absolute optical instruments [5] where all light rays form circular trajectories and where every point in space is

stigmatically imaged. In 2009 Leonhardt hypothesised [3] that this imaging can be perfect even for waves and is not limited by diffraction, enabling in principle super-resolution imaging. This result started a hot scientific debate and opened a rich area of research exploration, with many theoretical and experimental results both supporting [6–10] and opposing [9, 11–14] the claim. During the discussion it turned out that a central notion in answering the question of whether one can achieve super-resolution with MFE and other absolute instruments, is the need for a drain (outlet) for the radiation [3, 15, 16] within the lens. Without the drain, imaging is diffraction limited due to the interference of incoming converging waves and outgoing waves [13, 17] at the image point. The question that stands now is how such a drain could be practically employed to achieve super-resolution in microscopy, nanolithography, etc.

To say that something has perfect resolution, it is a necessary condition that one be able to resolve two closely spaced point sources in the image, even if the separation of the sources is much smaller than the wavelength. Is this possible for MFE? The unique property of MFE (as well as many other absolute instruments) is that all rays emerging from a point necessarily pass stigmatically through its corresponding image point. This means that power released from a point can only be fully absorbed at its image point, suggesting that imaging by MFE should be perfect. If one were to have a 'perfect drain' which could be scanned across the image space of the fisheye without prior knowledge of the location of a single source, there would be only a single point where all the power would flow continuously into the drain. For all other points, some power would not be absorbed and excess energy would remain in the device, which could then disclose that the position of the drain is 'wrong'. One could then hope that this information would provide an unlimited resolution of the location of the source.

It has turned out that it is not easy to construct such an ideal passive drain, either theoretically or practically. One option could be artificial black holes [18], but this would require rather extreme optical media; another option would be a drain adapted to a particular position within MFE [15]. Because of the general difficulty of designing a passive drain which could be used to test the MFE in all circumstances, however, we sidestep the issues of constructing a perfect passive drain and instead construct a theoretically perfect active drain. This will be accomplished by physically placing an active infinitesimal dipole antenna at the drain point and determining the theoretically most perfect antenna current to absorb the maximum power, for any given time-dependent current at the source(s). A passive drain would do no better than this in terms of absorption or resolution, since it would have to interact with the same set of modes of the fisheye as an active drain. Then, with our theoretically perfect drain, we will examine what happens when it is misplaced from the image point in terms of residual power in the fisheye. Based on this, we will make a conclusion about perfect imaging in the MFE with such an active drain that, most likely, applies to passive drains as well.

The paper is organised as follows: in the next section we demonstrate the well-known equivalence of waves in MFE and on a 2D sphere. In section 3 we discuss expansion of a wave on the sphere into modes and the energy in the wave; in section 4 we propose the optimal active drain. In section 5 we analyse the resolution that can be achieved with this drain theoretically and in section 6 by wave simulations. We conclude in section 7.

2. Equivalence of 2D MFE and an optically homogeneous sphere

In the following we will consider a two-dimensional Maxwell's fisheye of unit radius. Its refractive index depends only on the distance r from the origin and is given by the well-known formula

$$n_{\mathrm{MFE}}(r) = \frac{2}{1 + r^2}. \tag{1}$$

It has been shown by Luneburg [19] that within geometrical optics, the ray propagation in this device is equivalent to ray propagation on a homogeneous sphere with unit radius and unit refractive index. Ray trajectories in the plane of MFE are obtained by mapping the ray trajectories on the sphere, the great circles, via the stereographic projection [20]. This beautiful relationship between wave propagation in a 2D MFE and wave propagation on a sphere can be regarded as a precursor of transformation optics.

Interestingly, the Luneburg relationship is valid not only for rays but also for waves in MFE if the scalar wave equation is considered. It is a consequence of the fact that the stereographic projection is a conformal mapping, and of the properties of the Laplace operator in such a transformation. To show this, we write the wave equation for scalar waves in the 2D MFE in the absence of sources

$$\Delta_{(r,\varphi)} u - n_{\mathrm{MFE}}^2 \frac{\partial^2 u}{\partial t^2} = 0, \tag{2}$$

where $\Delta_{(r,\varphi)}$ denotes the Laplace operator in polar coordinates (r, φ). Here we are using units in which the speed of the waves is equal to unity for $n = 1$. We now transform this equation to new coordinates (θ, ϕ) parameterising a unit sphere which is stereographically projected onto the plane (r, φ). The relations between the coordinates (θ, ϕ) and (r, φ) are

$$r = \cot \frac{\theta}{2}, \qquad \varphi = \phi. \tag{3}$$

Written in the new coordinates, equation (2) becomes

$$\Delta_{(\theta,\phi)} u - \frac{\partial^2 u}{\partial t^2} = 0, \tag{4}$$

where

$$\Delta_{(\theta,\phi)} = \frac{1}{\sin \theta} \frac{\partial}{\partial \theta} \left(\sin \theta \frac{\partial}{\partial \theta} \right) + \frac{1}{\sin^2 \theta} \frac{\partial^2}{\partial \phi^2} \tag{5}$$

is the angular part of the Laplace operator in spherical coordinates. This way equation (4) describes waves propagating on a unit sphere with a unit refractive index and hence also unit speed. We will call the sphere 'virtual space' using terminology of transformation optics.

From now on we will consider only waves on the sphere. Thanks to its equivalence with the 2D MFE, the results will apply to that case also.

3. Mode expansion of a wave on the sphere

Any wave on the unit sphere (or in the equivalent MFE) at any moment of time can be described by a superposition of eigenmodes. Separating the time variables in equation (4) in terms of the factor $\exp\left(\pm\mathrm{i}\omega t\right)$, we arrive at the Helmholtz equation in spherical coordinates $\left(\theta, \varphi\right)$ for the spatial part of u, whose solutions are the spherical harmonics

$$Y_{lm}\left(\theta, \phi\right) = N_{lm}\mathrm{e}^{\mathrm{i}m\phi}P_l^m\left(\cos\theta\right), \quad m = 0, \pm 1, ..., \pm l, \tag{6}$$

where $P_l^m\left(z\right)$ are associated Legendre polynomials and N_{lm} are normalisation factors. The corresponding eigenfrequencies $\omega_{lm} = \omega_l = \sqrt{l\left(l+1\right)}$ are degenerate with respect to m. This is a consequence of the high symmetry of the sphere but is also a demonstration of the fact that MFE is an absolute instrument [21, 22]. The modes in the corresponding MFE are obtained by combining equations (6) and (3), i.e., by $Y_{lm}\left(2\,\mathrm{arccot}\,r, \varphi\right)$. Thanks to the degeneracy, the choice of the modes (6) is not unique. We could use, for example, modes Y'_{lm} that would be obtained from (6) by an arbitrary 3D rotation. The relation between the old and new modes would then be given by the SU(2) Wigner rotation matrices $d^l_{mm'}$ [23]. This way, a general wave on the sphere can be expressed as a superposition

$$u\left(\theta, \phi, t\right) = \sum_{l=0}^{\infty}\sum_{m=-l}^{l} c_{lm}\left(t\right)Y_{lm}\left(\theta, \phi\right). \tag{7}$$

In the absence of sources, each coefficient $c_{lm}\left(t\right)$ simply oscillates at its frequency ω_l. However, we will be interested in a situation in which the wave is a result of an action of sources on the sphere. Mathematically this corresponds to replacing the zero on the right-hand side of equation (4) by a source function $q\left(\theta, \phi, t\right)$ describing the action of the sources. In the situation in which there is no wave on the sphere at time $t \to -\infty$, i.e., the entire wave is a result of the action of the sources, the coefficients c_{lm} can be expressed with the help of [21], equation (6) as

$$c_{lm}\left(t\right) = \frac{1}{\omega_l}\int_{-\infty}^{t} \mathrm{d}t'\,\sin\left[\omega_l\left(t-t'\right)\right]\int_{\Omega}\mathrm{d}\Omega\,Y_{lm}^*\left(\theta, \phi\right)q\left(\theta, \phi, t'\right), \tag{8}$$

where Ω and $\mathrm{d}\Omega = \sin\theta\,\mathrm{d}\theta\,\mathrm{d}\phi$ denote the surface of the unit sphere and its differential, respectively.

Another useful quantity that we will need is the total energy of the wave. It can be derived by the standard method from the Lagrangian

$$L = \frac{A}{2}\int_{\Omega}\left(\left|\dot{u}\right|^2 - \left|\nabla u\right|^2\right)\mathrm{d}\Omega, \tag{9}$$

where A is a constant, that leads to the wave equation (4); the dot here denotes the partial time derivative. The energy is then

$$E = \frac{A}{2}\int_{\Omega}\left(\left|\dot{u}\right|^2 + \left|\nabla u\right|^2\right)\mathrm{d}\Omega = \frac{A}{2}\sum_{l=0}^{\infty}\sum_{m=-l}^{l}\left(\left|\dot{c}_{lm}\right|^2 + \omega_l^2\left|c_{lm}\right|^2\right) \tag{10}$$

where we have used the expansion (7) and the orthonormality of the modes. Using equation (8), we find after some algebra that

$$E\left(t\right) = \frac{A}{4} \sum_{l=0}^{\infty} \sum_{m=-l}^{l} \left(\left|Q_{lm}\left(\omega_l, t\right)\right|^2 + \left|Q_{lm}\left(-\omega_l, t\right)\right|^2\right), \tag{11}$$

where we have defined

$$Q_{lm}\left(\omega, t\right) = \int_{-\infty}^{t} \mathrm{d}t' \ \mathrm{e}^{\mathrm{i}\omega t'} \int_{\Omega} \mathrm{d}\Omega \ Y_{lm}^*\left(\theta, \phi\right) q\left(\theta, \phi, t'\right). \tag{12}$$

4. Optimal active drain

We will now proceed to describing the emission of a wave on the sphere and its absorption by an optimal active drain. Suppose a wave (typically a pulse) is emitted from a point A. We will then design an active source at another point B that absorbs as much of the energy of the pulse from A as possible. As we will see, it is only possible to absorb all the energy if B is an image of A, i.e., if the points A and B either coincide or are placed opposite each other on the sphere. At the same time, even if B is not an image of A, it is still possible to absorb some energy. How this amount of maximally absorbed energy depends on the distance of B from the image of A can provide a measure of spatial resolution of MFE: for example, if the amount of energy that can be absorbed drops very quickly with the separation of B from the image point, it would imply that the spatial resolution is very high, and vice versa.

We will describe the emission and absorption using the source function $q\left(\theta, \phi, t\right)$ defined in the previous section. The emission will correspond to a function $\delta_A(\theta, \phi) h_A(t)$, where $\delta_A\left(\theta, \phi\right)$ denotes a spatial Dirac δ-function whose integral over the sphere is unity and that is zero everywhere with the exception of the point A,[3] and $h_A(t)$ describes the temporal part of the source action (for example, the current at point A as a function of time). Similarly, the full or partial absorption of the wave at point B is achieved by a source function $\delta_B\left(\theta, \phi\right) h_B\left(t\right)$ on the right-hand side of equation (4). Without loss of generality, we can assume that point B is located at the north pole ($\theta = 0, \phi = 0$) because the spherical coordinate system (and the modes along with it) can always be rotated such that point B has this position. For the same reason, we can assume that point A has coordinates $\left(\theta = \theta_A, \phi = 0\right)$, see figure 1(a).

Now, when a wave is emitted from point A, in principle all possible modes of the sphere can be excited with the exception of the modes $Y_{lm}\left(\theta, \phi\right)$ that have a node at A—for these latter modes the integral over the sphere in equation (8) is zero and so are the corresponding coefficients c_{lm}. Similarly, the active drain at point B can absorb the energy only from modes that are nonzero at B. Since B is placed at the north pole where only the modes with $m = 0$ are nonzero, it is the energy from only these modes that can be absorbed there; the energy in all the remaining modes (those with $m \neq 0$) will stay in the device no matter what function $h_B\left(t\right)$ we may choose. This means that the largest amount of energy will be extracted if we choose the function $h_B\left(t\right)$ such that all coefficients $c_{l0}\left(t\right)$ go to zero for $t \to \infty$. As we show in the Appendix, this is indeed possible to achieve. This naturally leads to the definition of an optimal active drain placed on the north pole (or the south pole) of the sphere: it is a drain that extracts

---

[3] If A has coordinates $\left(\theta_A, \phi_A\right)$ and if $\sin \theta_A \neq 0$, then $\delta_A\left(\theta, \phi\right)$ can be expressed as $\delta\left(\theta - \theta_A\right) \delta\left(\phi - \phi_A\right) / \sin \theta_A$.
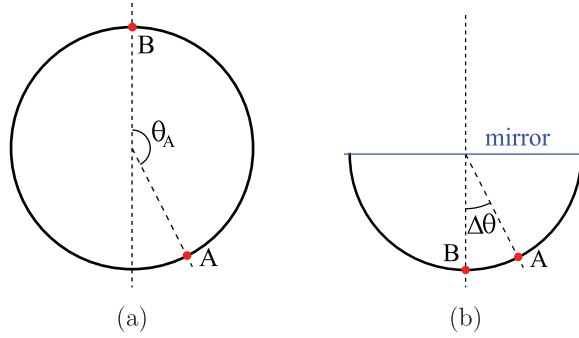
Figure 1. (a) The position of the source A and the drain B on the sphere corresponding to MFE. Only the cut with the plane $\phi = 0$, $\phi = \pi$ is shown. (b) The same for the hemisphere corresponding to MFEM; the drain position is now mirror-imaged to the South pole.

all the energy from modes Y_{l0} and leaves the energy only in the modes Y_{lm} with $m \neq 0$. An optimal active drain placed at some general point C on the sphere would be defined in an analogous way, but instead of Y_{lm}, we would use the rotated modes Y'_{lm} mentioned in section 3 whose axis of symmetry passes through point C.

5. Resolution with the optimal active drain

As we have seen in the previous section, only the modes with $m = 0$ can be de-excited by a drain B placed at the north pole. An important question is how much energy can be absorbed by this optimal drain, and how this amount depends on the key parameter θ_A, i.e., on the offset of the drain from the 'correct' image position of source A.

To answer this question, we have to calculate the total energy E_A in the system as a result of the action of the emission function h_A only and compare it with its portion E'_A that can be absorbed by the optimal drain. As we have seen, the latter energy corresponds only to the modes with zero m. The energy E_A can be calculated with the help of equations (11) and (12), where we use the source function $q(\theta, \phi, t) = \delta_A(\theta, \phi) h_A(t)$ and set $t \to \infty$. We then get for $Q_{lm}(\omega_l, t \to \infty)$

$$Q_{lm}(\omega, t \to \infty) = N_{lm} P_l^m(\cos\theta_A) \int_{-\infty}^{\infty} e^{i\omega t'} h_A(t') \, dt'. \tag{13}$$

If we denote the time integral by $\tilde{h}_A(\omega)$, the energy becomes

$$E_A = \frac{A}{4} \sum_{l=0}^{\infty} \sum_{m=-l}^{l} \left[N_{lm} P_l^m(\cos\theta_A) \right]^2 \left[\left| \tilde{h}_A(\omega_l) \right|^2 + \left| \tilde{h}_A(-\omega_l) \right|^2 \right]. \tag{14}$$

The energy E'_A would be described similarly as E_A, but with the value of m fixed to zero for each l.

We will now define a quantity $\eta(\theta_A)$ as the ratio of the energy E'_A that can be extracted from the system by the optimal drain and the energy E_A that was input to the system by the
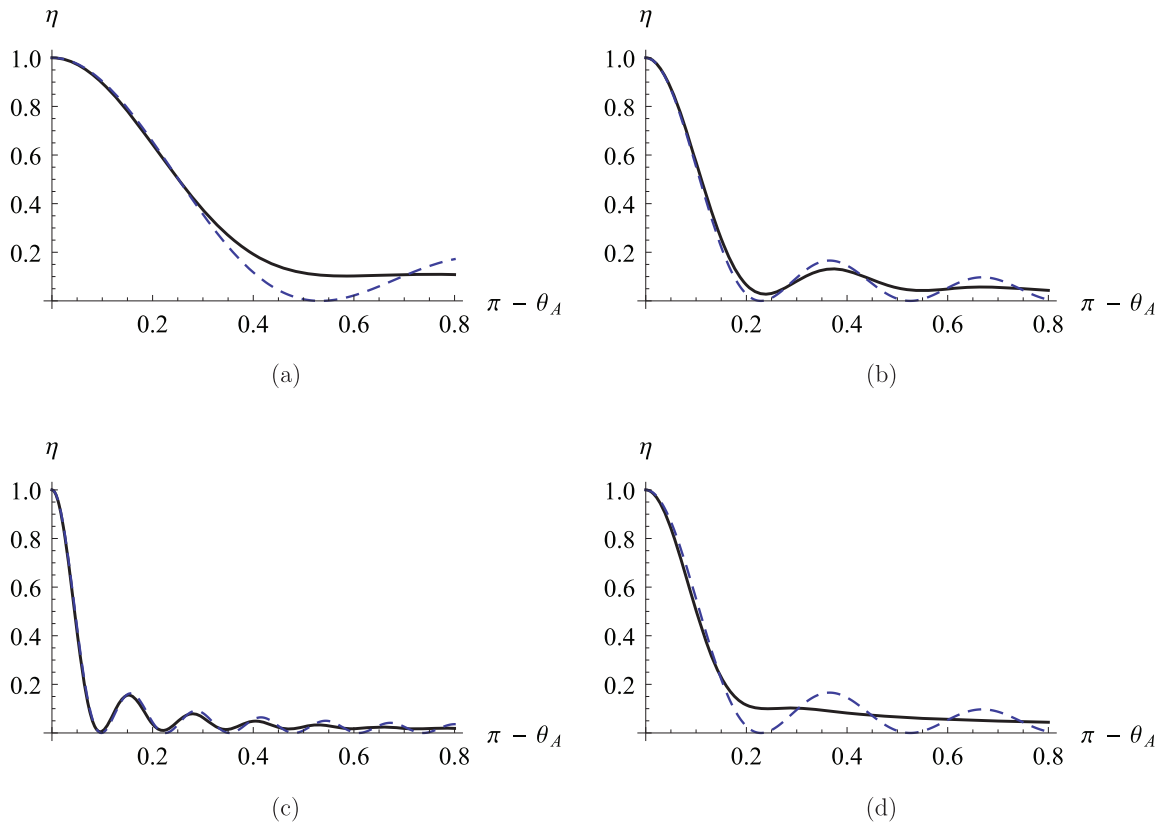
source:

$$\eta\left(\theta_{\mathrm{A}}\right) = \frac{E_{\mathrm{A}}'}{E_{\mathrm{A}}} = \frac{\sum_{l=0}^{\infty}\left[N_{l0}P_l^0\left(\cos\theta_{\mathrm{A}}\right)\right]^2\left[\left|\tilde{h}_{\mathrm{A}}\left(\omega_l\right)\right|^2 + \left|\tilde{h}_{\mathrm{A}}\left(-\omega_l\right)\right|^2\right]}{\sum_{l=0}^{\infty}\sum_{m=-l}^{l}\left[N_{lm}P_l^m\left(\cos\theta_{\mathrm{A}}\right)\right]^2\left[\left|\tilde{h}_{\mathrm{A}}\left(\omega_l\right)\right|^2 + \left|\tilde{h}_{\mathrm{A}}\left(-\omega_l\right)\right|^2\right]}. \quad (15)$$

Apparently, $\eta(0) = \eta(\pi) = 1$ because the associated Legendre polynomials $P_l^m(\pm 1)$ become zero for $m \neq 0$. This expresses the fact that if the source is placed at either of the poles of the sphere, the energy can be completely extracted by a drain placed at either pole as well. If, however, θ_{A} differs from 0 or π, $\eta(\theta_{\mathrm{A}})$ becomes smaller than one, so some energy is left in the system. The key question is now how much energy can be absorbed in case of a subwavelength displacement. The answer depends on how steeply $\eta(\theta_{\mathrm{A}})$ changes with θ_{A} near 0 and π. Figure 2 shows the function $\eta(\theta_{\mathrm{A}})$ near $\theta_{\mathrm{A}} = \pi$ for a Gaussian emission pulse $\tilde{h}_{\mathrm{A}}(\omega) = \exp\left[-(\omega - \omega_0)^2/(2\Delta\omega^2)\right]$ with a few combinations of mean frequency ω_0 and frequency width $\Delta\omega$. (Note that on the horizontal axis there is the difference $\pi - \theta_{\mathrm{A}}$ expressing the offset of the drain from the right image position.) To judge whether the region where the energy can be efficiently absorbed is diffraction limited or not, we compare the width of the peak of $\eta(\theta_{\mathrm{A}})$ with the width of the peak of the spherical harmonic Y_{l_00} with l_0 chosen such that it corresponds best to the mean frequency ω_0 (i.e., l_0 gives the best approximation of $\omega_0 \approx \sqrt{l_0(l_0 + 1)}$). The latter width determines the size of the diffraction limited spot of a focused wave with frequency near ω_0. For this purpose, in figure 2 we compare $\eta(\theta_{\mathrm{A}})$ with the function $y_{l_0}(\theta_{\mathrm{A}}) \equiv \left[Y_{l_00}(\theta_{\mathrm{A}}, 0)/Y_{l_00}(0, 0)\right]^2$; the scaling factor ensures that $y_{l_0}(0) = y_{l_0}(\pi) = 1$. As figure 2 reveals, the functions $\eta(\theta_{\mathrm{A}})$ and $y_{l_0}(\theta_{\mathrm{A}})$ are very close, almost identical near $\theta_{\mathrm{A}} = \pi$ (and the same is true near $\theta_{\mathrm{A}} = 0$). This unfortunately means that the region of efficient absorption is diffraction limited. In other words, to make $\eta(\theta_{\mathrm{A}})$ significantly smaller than unity, we must shift the drain from the image position by a distance comparable with a wavelength. This means that the optimal active drain cannot resolve the position of the source with better than diffraction-limited resolution.

A similar behaviour in $\eta(\theta_{\mathrm{A}})$ can be observed if we instead consider a quantity $\eta_l(\theta_{\mathrm{A}})$ corresponding to the modes of one particular value of l (and hence one frequency) by omitting the sums over l in equation (15):

$$\eta_l\left(\theta_{\mathrm{A}}\right) = \frac{\left[N_{l0}P_l^0\left(\cos\left(\theta_{\mathrm{A}}\right)\right)\right]^2}{\sum_{m=-l}^{l}\left[N_{lm}P_l^m\left(\cos\left(\theta_{\mathrm{A}}\right)\right)\right]^2}. \quad (16)$$

This corresponds to the ratio of energies with and without the drain action, but just for the modes with a given frequency ω_l. It turns out that the function $\eta_l(\theta_{\mathrm{A}})$ is practically indistinguishable from the function $y_l(\theta_{\mathrm{A}})$, which leads to the same conclusion about the resolution with the optimal active drain as for Gaussian pulses.

Figure 2. The function $\eta\left(\theta_{\mathrm{A}}\right)$ for Gaussian source functions $h_{\mathrm{A}}\left(t\right)$ with several values of the mean frequency ω_0 and width $\Delta\omega$. On the horizontal axis there is the difference $\pi - \theta_{\mathrm{A}}$. For comparison, the dashed curves show the scaled square of the spherical harmonic $Y_{l_0 0}\left(\theta_{\mathrm{A}}, 0\right)^2$ with l_0 being the integer that gives the best approximation $\omega_0 \approx \sqrt{l_0\left(l_0 + 1\right)}$, and the scaling ensures that the value of the function is unity for $\theta_{\mathrm{A}} = 0$. The parameters are (a) $\omega_0 = 4$, $\Delta\omega = 2$, (b) $\omega_0 = 10$, $\Delta\omega = 2$, (c) $\omega_0 = 25$, $\Delta\omega = 2$, and (d) $\omega_0 = 10$, $\Delta\omega = 5$. We see that in all cases the width of the dip in the function $\eta\left(\theta_{\mathrm{A}}\right)$ corresponds very well to the width of the maximum of the spherical harmonic, showing that the absorption is efficient in the whole diffraction limited region.

6. Wave simulations

To verify our theoretical results described above, we performed simulations of a Gaussian pulse emission and absorption by the optimal drain. However, to make the medium finite, we used 2D Maxwell's fisheye mirror (MFEM) [2–4] instead of 2D MFE. It has the same refractive index (1) as MFE but the medium occupies just the unit disc instead of the whole plane and it is surrounded by a mirror at $r = 1$. Virtual space for MFEM is the southern hemisphere corresponding to the interval $\theta \in \left[\pi/2, \pi\right]$ with a mirror along the equator, see figure 1(b). The modes in MFEM are the same as those in MFE, but only those combinations $\{l, m\}$ for which $l - m$ is odd are allowed due to the boundary condition at the mirror. While in MFE the image
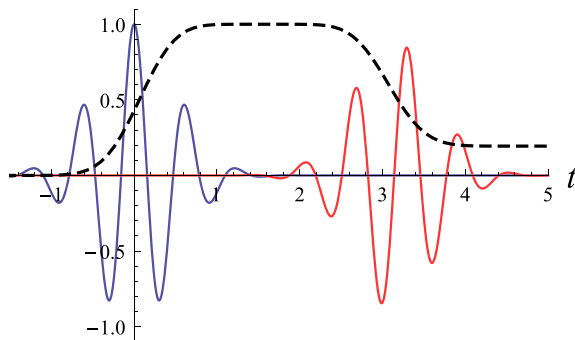
Figure 3. A Gaussian source pulse (blue, the first wave packet), the corresponding optimal drain pulse (red, the second wave packet) and the energy in the system (dashed black) as a function of time for the parameters $\omega_0 = 10$, $\Delta\omega = 2$ and $\theta_A = \lambda/10$. Although the drain is misplaced by $\Delta\theta = \lambda/10$ from the image position, still most (over 80%) of the injected energy can be extracted.

position is given by the inversion in the unit sphere, in MFEM a point at position $\vec{r}$ is imaged to the point $-\vec{r}$ [2, 3].

In our simulations (see animations 1 and 2 in supplementary data), the source was placed at the point $\left(r = \cot\left[\theta_A/2\right], \varphi = 0 \right)$ that is imaged to the point $\left(r = \cot\left[\theta_A/2\right], \varphi = \pi \right)$; the drain was placed at the centre that corresponds to $\theta_B = \pi$. This way the displacement of the drain from the right image position in virtual space is $\Delta\theta = \pi - \theta_A$. For the purpose of the animations, we calculated the drain pulse by the procedure shown in the Appendix, and then, for a given moment in time, we calculated the coefficients of the individual modes using equation (8), and the corresponding energy in the system. In figure 3 we show a particular example of the source pulse, the corresponding optimal drain pulse and the energy as a function of time for $\omega_0 = 10$, $\Delta\omega = 2$ and $\Delta\theta = \lambda/10$ (with $\lambda = 2\pi/\omega_0$). We see that after the drain pulse is finished, most of the energy was absorbed even though the drain was displaced from the correct position by $\lambda/10$. The ratio of the absorbed and injected energy obtained from the simulation was 0.8061, which is in a good agreement with equation (15), which yields $\eta(\theta_A) = 0.8076$ for the same situation. Animation 1 shows the evolution of the wave; the bar on the right-hand side shows the actual energy in the system. Animation 2 shows the same, but for a larger displacement $\Delta\theta = \lambda/5$. In this case the optimal active drain absorbs approximately 40% of the injected energy.

7. Conclusion

We have analysed the absorption of a pulse in an absolute optical instrument, Maxwell's fisheye, by an optimal active drain placed in a general position with respect to a source. We have shown that even if the drain is placed at a 'wrong' place, a certain amount of energy can still be extracted. For Gaussian or monochromatic pulses, the dependence of this energy on the displacement very closely mimics the square of the absolute value of the spherical harmonic describing the wave at the corresponding mean frequency, with the maximum at the actual image point. This shows that the spot where the energy can efficiently be absorbed is diffraction limited, and therefore in this configuration Maxwell's fisheye unfortunately cannot provide

super-resolution. Our results may contribute to the growing belief that subwavelength imaging with absolute instruments will not be practically possible.

Acknowledgements

Appendix

To express the coefficients c_{lm} in a situation where a pulse $h_A(t)$ is emitted from point A and a part of it is absorbed at point B via a drain pulse $h_B(t)$, we use the source function $q(\theta, \phi, t) = \delta_A(\theta, \phi)h_A(t) + \delta_B(\theta, \phi)h_B(t)$ in equation (8). Employing the special choice of the positions of the points A and B (in particular, $\theta_B = 0$, $\phi_A = \phi_B = 0$), and integrating over the sphere Ω, we get

$$c_{lm}(t) = \frac{N_{lm}}{\omega_l} \int_{-\infty}^{t} \sin\left[\omega_l(t - t')\right] \left[P_l^m(\cos\theta_A)h_A(t') + P_l^m(1)h_B(t')\right] dt' \tag{A1}$$

Taking into account that for $m \neq 0$ it holds that $P_l^m(1) = 0$, we see from equation (A1) that for these modes the function $h_B(t)$ indeed has no influence on $c_{lm}(t)$, and therefore no energy can be extracted by the active (as well as passive, of course) drain from these modes.

To extract the energy from the modes with $m = 0$, we need to make sure that $c_{l0}(t) \to 0$ for $t \to \infty$ for all l. We see from equation (A1) that this will be true if the Fourier transform of the brackets expressed at any of the eigenfrequencies ω_l or their negative counterparts $-\omega_l$ is zero. Using the fact that $P_l^0(1) = 1$ for all l, we find that the condition $c_{l0} = 0$ becomes

$$\int_{-\infty}^{\infty} e^{\pm i\omega_l t}\left[P_l(\cos\theta_A)h_A(t) + h_B(t)\right] dt = 0, \qquad l = 0, 1, 2, \ldots \tag{A2}$$

The function $h_A(t)$ is given by the emission pulse, and the task is to find a function $h_B(t)$ for which the condition (A2) is satisfied. This function is not unique; in fact, there are infinitely many such functions.

To find them, we introduce the Fourier transforms of the source and drain functions as follows:

$$\tilde{h}_{A,B}(\omega) = \frac{1}{\sqrt{2\pi}} \int_{-\infty}^{\infty} e^{i\omega t}h_{A,B}(t)\, dt\,, \qquad h_{A,B}(t) = \frac{1}{\sqrt{2\pi}} \int_{-\infty}^{\infty} e^{-i\omega t}\tilde{h}_{A,B}(\omega)\, d\omega \tag{A3}$$

For a given source pulse described by $h_A(t)$, or, equivalently, by $\tilde{h}_A(\omega)$, the most general form of the drain pulse is

$$\tilde{h}_{\text{B}}(\omega) = -\frac{P^0_{\ell(\omega)}(\cos\theta_{\text{A}})}{P^0_{\ell(\omega)}(1)}\,\tilde{h}_{\text{A}}(\omega)f(\omega). \tag{A4}$$

Here $f(\omega)$ is an arbitrary function that satisfies $f(\pm\omega_l)=1$ for all l and we have defined the function $\ell(\omega)=\sqrt{\omega^2+1/4}-1/2$; for positive ω it is the inverse function of $\omega(\ell)=\sqrt{\ell(\ell+1)}$ that gives the eigenfrequencies of MFE for integers ℓ, and for negative ω it is defined such that $\ell(\omega)=\ell(|\omega|)$. This ensures that $\ell(\pm\omega_l)=l$, and it can be easily verified by combining equations (A2), (A3) and (A4) that the drain pulse described by equation (A4) really has the desired properties. The function $f(\omega)$ can be used to manipulate the shape of the drain pulse. For example, using $f(\omega)=\text{e}^{2\text{i}\pi\ell(\omega)}$ in case of a quasi-monochromatic Gaussian pulse causes a shift of the drain pulse by 2π in time accompanied with a slight shape change due to dispersion.

References

[1] Maxwell J C 1854 *Camb. Dublin Math. J.* **8** 188
[2] Miñano J C 2006 *Opt. Express* **14** 9627
[3] Leonhardt U 2009 *New J. Phys.* **11** 093040
[4] Tyc T, Herzánová L, Šarbort M and Bering K 2011 *New J. Phys.* **13** 115004
[5] Born M and Wolf E 2006 *Principles of Optics* (Cambridge: Cambridge University Press)
[6] Leonhardt U 2010 *New J. Phys.* **12** 058002
[7] Leonhardt U and Philbin T G 2010 *Phys. Rev.* A **81** 011804
[8] Ma Y G, Sahebdivan S, Ong C K, Tyc T and Leonhardt U 2011 *New J. Phys.* **13** 033016
[9] Tyc T and Zhang X 2011 *Nature* **480** 42
[10] Miñano J C, Marques R, González J C, Benítez P, Delgado V, Grabovickic D and Freire M 2011 *New J. Phys.* **13** 125009
[11] Blaikie R J 2010 *New J. Phys.* **12** 058001
[12] Kinsler P and Favaro A 2011 *New J. Phys.* **13** 028001
[13] Merlin R 2011 *J. Opt.* **13** 024017
[14] Quevedo-Teruel O, Mitchell-Thomas R C and Hao Y 2012 *Phys. Rev.* A **86** 053817
[15] González J C, Benítez P and Miñano J C 2011 *New J. Phys.* **13** 023038
[16] Ma Y, Wu T and Ong C K 2013 *J. Opt.* **15** 125705
[17] Tyc T 2012 *Opt. Lett.* **37** 924
[18] Narimanov E E and Kildishev A V 2009 *Appl. Phys. Lett.* **95** 041106
[19] Luneburg R K 1964 *Mathematical Theory of Optics* (Berkeley: University of California Press)
[20] Leonhardt U and Philbin T G 2009 *Prog. Opt.* **53** 69
[21] Tyc T and Danner A 2012 *New J. Phys.* **14** 085023
[22] Tyc T 2013 *New J. Phys.* **15** 065005
[23] Wigner E R 1931 *Gruppentheorie und ihre Anwendungen auf die Quantenmechanik der Atomspektren* (Braunschweig: Vieweg Verlag)